Norwegian University of Life Sciences
Faculty of Environmental Science and Technology
Department of Mathematical Sciences and Technology (IMT)

Master Thesis 2015
30 credits

Hyperspectral near infrared imaging of untreated aspen and adaptation of an existing mould prediction model.

Marcus Edward Helland

ACKNOWLEDGEMENTS

Thanks to:

Thomas Kringlebotn Thiis and Ingunn Burud for guidance and inspiring meetings.

Solrunn and Kärt for the visual mould measurements and experimental setup.

Lone Gobakken for experimental setup.

Geir and Sebastian for leaf moisture measurements.

My parents for support.

ABSTRACT

Wood as a building material is beneficial for the environment; it stores CO_2 and saves CO_2 emissions from other materials. Prediction models of mould growth are necessary to estimate the service life of wood. To make accurate models, accurate assessments are needed. Todays standard of visual assessment has some weaknesses, with different rating scales which can be difficult to compare and a subjective rating. Hyperspectral imaging may provide objective and accurate mould assessments for use in more accurate mould growth models.

Untreated wood samples were sprayed with a mould culture before exposed to eight different transient climates in a laboratory. Weekly measurements of mould growth was assessed by hyperspectral imaging and by visual method EN 927-3. Partial least squares discriminant analysis (PLS-DA) was used to differentiate and predict mould growth on samples. Mould growth intensity factor of aspen, with the empirical mould growth model by Viitanen and Hakku, was estimated and compared with measured mould growth.

Hyperspectral imaging consequently showed less mould than visual assessment. There was a large variation in mould growth on aspen under equal climate conditions. The growth intensity factor, k_1, for aspen in 25C, 85% relative humidity and 2 hours daily light showers, was calculated to $k_1 = 10 \pm 10$ for mould index larger than 1 and $k_1 = 0{,}9 \pm 0{,}2$ for mould index less than 1.

Hyperspectral images contain differences, in the spectral bands from 900nm to 1700nm, between untreated aspen and mould. This can be used to measure amount of mould on an untreated aspen cladding.

CONTENTS

Figure 0 Wooden cladding, northwest facing wall, Astrup Fearnley Museet. Dog pee has resulted in a "clean" look compared to the darker, mouldy wood.

1 INTRODUCTION

Wood is a renewable, environmentally friendly and CO_2 storing, and saving, building material. Untreated wooden cladding has become increasingly popular for its natural aesthetics and low maintenance. The natural grey colour an untreated wooden cladding develops over time, is a result of mould growth and degradation by sunlight. Often however, this development is uneven and is regarded a discolouring. Mould growth models may predict these discolourings (not the ones in Fig. 0), so they can be avoided. They may be a useful tool for architects when designing facades, and for estimating life cycle cost. The existing models use a visual method for measuring mould growth which is subjective and has several different rating scales which make them difficult to compare. A more accurate measurement method may give more accurate prediction models, which use percentages instead of a mould rating scale.

Hyperspectral imaging has already been applied to detect and quantify mould on wooden cladding by Burud et al, 2013 and 2015. These studies concluded that more research was necessary. This study will compare hyperspectral imaging to the visual assessment method, with the goal of finding an accurate and objective mould assessment method.

The second step is to adapt an existing model to aspen by finding the growth intensity factor, and comparing this to the measured values.

2 THEORY

2.1 FUNGUS

2.1.1 TYPES AND TROUBLES

Fungus belong to the kingdom of fungi, which includes yeast, mildew, moulds and mushrooms. Some types of fungi decay wood, and some do not. Brown rot, soft rot and white rot are types of wood decaying fungi, whilst mould normally only causes esthetical changes to wood (Byggforsk, Magnussen, 2007). Most decaying fungi also need more moisture over a longer period of time than mould to grow. The type this paper is concerned with is mould that only stains wooden cladding with a dark grey.

The dark colour, which can be seen with the naked eye, is often spores, but can also be mycelium, which consists of networks of tubular hyphae. Hyphae are very small, from 0,5um to 20um, so magnification is needed to see the individual hyphae. Spores are formed from hyphae and are carried away with air currents so the fungus can reproduce elsewhere. These spores are in the air everywhere and can be dormant from days to months (Cochrane, 1958). If spores germinate under good conditions, hyphae grow quick and can be visible within a week (Edvardsen and Ramstad, 2012 Trehusboka)

Growth needs for fungus are mainly water, oxygen, temperatures 0^{o}C to 45^{o}C, digestible substrate, and pH3 to 6. For mould to grow on wood the main dependencies are relative humidity (RH), temperature and the surface quality (Viitanen, 1994). Enough water for growth can be obtained from the air when relative humidity is above 80%. If temperatures are between +5^{o}C and + 50^{o}C and RH > 80%, the conditions are good enough for mould growth on pine and spruce sapwood (Viitanen, 1994). Growth is fast under conditions with RH of 95-98% and temperatures +20^{o}C to +40^{o}C, on untreated pine and spruce sapwood (Viitanen, 1994).

Under normal circumstances however, temperature and humidity fluctuate. A lab study with fluctuating conditions, with RH alternating between 90% and 60%, showed mould growth is slower compared to steady state conditions. Mould growth was found to be dependent on both the favourable and unfavourable RH conditions, and

not the mean RH value. Fluctuating temperatures between 22°C and 5°C had less effect than alternating RH, and mean temperatures could be used in prediction (Johansson, 2013).

Mould does not decay wood like rot fungi, but stained wood is more permeable and is not recommended for load bearing constructions (Zabel and Morel, 1992, p. 336). Indoors, mould is a problem because of the discolouring, the smell, it can be a sign of water leakage, and high concentrations of spores can lead to health problems. Outdoors, mould can give an undesired dirty look to a painted wooden facade, but on an untreated wooden cladding, it can give a desired effect.

There are various species of mould that stain wood, the most common one is *Aureobasidium pullulans.* Other genera of mould that also stain wood are *Aspergillus, Chaetomium, Cladosporium, Penicillium, Stachybotrys, Tricoderma and Ulocladium* (Mattsson,2004).

The problem with mould on untreated wooden cladding is the uneven staining, see Fig. 6. The uneven staining can be difficult to predict and can give unintended colouring effects to a facade.

These stains or discolourations are sometimes unwanted and sometimes a desired effect. Blue stain or sapstain are caused by fungi with pigmented hyphae and give a blue discolouration, which can often afflict pine sapwood and other sapwoods.

2.1.2 Detection and measurement

Mould is often first detected by the distinctive smell, but can also be seen with the naked eye. When measuring mould growth, a specific method must be used.

The Norwegian and European Standard EN 16492:2014 contains an assessment method for mould growth which uses a rating scale, table A.3 in the standard and Table 1 in this paper. This method is done with the naked eye and a microscope is only used to exclude other particles than mould. The rating scale is the standard for "Evaluation of surface disfigurement caused by fungi and algae on coatings" (NS-EN

16492:2014 p. 1) and was assumed to also be suitable for untreated wooden surfaces.

This rating scale has large margins of error in percentage and is a subjective method, as two people evaluating may estimate different ratings.

Table 1 Rating scale for mould growth from to NS-EN 16492:2014, table A.3

Rating	Percentage area of disfigurements
0	No growth on the surface of the specimen
1	Up to 10% growth on the surface of the specimen
2	More than 10% up to 30% growth on the surface of the specimen
3	More than 30% up to 50% growth on the specimen
4	More than 50% up to 100% growth on the specimen

The mould growth model by Hukka and Viitanen (1999, see 2.1.3) used a slightly different scale for measuring mould growth. This model uses a mould index, shown in Table 2, which includes the use of a microscope. This was necessary to find the growth intensity factor k_1 because it relies on the difference from when mould is visible in a microscope, mould index 1, to when it is visible to the naked eye, mould index 3.

Table 2 Mould index developed by Viitanen and Hukka, 1999 and updated by Ojanen et al in 2010.

Index	Description of Growth Rate
0	No growth
1	Small amounts of mould on surface (microscope), initial stages of local growth
2	Several local mold growth colonies on surface (microscope)
3	Visual findings of mold on surface, < 10% coverage, or < 50% coverage of mold (microscope)
4	Visual findings of mold on surface, 10%–50% coverage, or > 50% coverage of mold (microscope)
5	Plenty of growth on surface, > 50% coverage (visual)
6	Heavy and tight growth, coverage about 100%

Other mould growth rating scales also exist, for example the one Thelandersson used in 2013, which only describes growth with adjectives such as sparse, patchy and heavy. A more accurate method of quantifying mould growth is desired to make prediction models of mould growth on facades. Both of these methods are inaccurate when above 10% mould coverage, and they may be too subjective (Bardage, 2004; Van den Bulcke et al., 2005; Van den Bulcke et al., 2006). They also depend on experienced personnel and comparisons made by different laboratories can be difficult (Bardage, 2004). Van den Bulcke, 2005 and 2006, used image processing as an alternative to visual assessment of blues stain fungi with good results.

More recently, Burud et al, 2013, 2015 used hyperspectral imaging and Principle Component Analysis (PCA) and partial least squares discriminant analysis (PLS-DA) to detect and quantify blue stain fungi. This method gives the amount of mould coverage directly as a percentage, which is easier for anyone to relate to, and potentially more precise, than a mould rating. The PCA technique was able to extract the fungal signal better with near infrared (NIR) spectrum images than with simple RGB images, which indicated that fungus has other spectral signals than the visible colour.

2.1.3 MOULD GROWTH MODELS

Modelling the mould growth allows predictions of where and when mould will grow. This can be a useful tool for predicting service life, and for architects when designing facades, of wooden cladding.

Many mould growth models have been described and developed, for example the isopleth systems, biohygrothermal model, condensation targeter, empirical VTT model and time-of-wetness (Adan 1994, Hukka & Viitanen 1999, Johannsson et al 2010, Krus et al 2007, Sedlbauer 2002). Relative humidity and surface temperature are included as they are the most important factors in these models. Time is also important, and not included in all these models. A model by Gobakken et al. (2010)

used the number of hours the relative humidity was above 80% concurrently with temperature above 5°C, to make prediction models of mould growth.

The empirical mould growth model developed by Viitanen and Hukka in 1999, was based on laboratory studies of northern wood species. The model was made by using regression analysis of the measured data and gives the mould growth as a mould index. This mould index is used when measuring mould growth and is then set to an integer value from 0 to 6, see Table 2, the model however gives the mould index with decimals. With this model, predictions of mould growth can be made from known relative humidity, temperature and time under constant or fluctuating conditions.

This model was updated by Ojanen et al in 2010, to be able to analyse other building materials such as concrete, glass wool and EPS. This updated Valtion Teknillinen Tutkimuskeskus (VTT) model for wood used the differential equation:

$$\frac{dM}{dt} = \frac{1}{7 \times \exp(-0.68\ln T - 13.9\ln RH + 0.14W - 0.33SQ + 66.02} \, k_1 k_2 \qquad (1)$$

dM is the change in mould index, see fig , *dt* is the change in time in days, *T* is the temperature, *RH* is the relative humidity. *SQ* is the surface quality of the wood, *SQ* = 0 for sawn wood and *SQ*=1 for kiln-dried. For material other than wood, *SQ* = 0 is used. W denotes timber species, *W* = 0 for pine and *W* = 1 for spruce. k_1 is the growth intensity factor depending on material, see eq. (5) and k_2 is a moderation of k_1 when the mould index approaches the maximum value in the existing conditions, calculated with:

$$k_2 = \max\left[1 - exp\left(2.3 \cdot (M - M_{max})\right), 0\right] \qquad (2)$$

where *M* is the mould index and M_{max} is the maximum mould index value in the existing conditions.

M_{max} was calculated with:

$$M_{max} = A + B \cdot \frac{RH_{crit} - RH}{RH_{crit} - 100} - C \cdot \left(\frac{RH_{crit} - RH}{RH_{crit} - 100}\right)^2 \quad (3)$$

here RH is the relative humidity of the air, RH_{crit} is the lowest relative humidity in which mould will start to grow. M_{max} is the maximum mould index value in the existing conditions. A, B and C are coefficients depending on the material and are estimated from experiments under constant temperature and RH conditions. For pine, and similar materials in the "very sensitive" class in Fig. 1, their approximations were A = 1, B = 7 and C = 2.

RH_{crit} was estimated from constant humidity condition experiments and depends on the temperature:

$$RH_{crit} = \begin{cases} -0.00267T^3 + 0.160T^2 - 3.13T + 100.0, & \text{when } T \leq 20 \\ RH_{min}, & \text{when } T > 20 \end{cases} \quad (4)$$

Here RH_{crit} is the critical, lowest relative humidity for mould to grow, and T is the air temperature. RH_{min} was set to 80% for wood and wood-based products. k_1 is as described earlier, a growth intensity factor, this factor is also a key when translating the model for different materials. The reference material was pine sapwood, so measurements of pine are needed in addition to the new material desired modelled.

The k_1 factor is calculated:

$$k_1 = \frac{t_{M=1,pine}}{t_{M=1}} \qquad \text{when } M < 1 \tag{5}$$

$$k_1 = 2 \cdot \frac{(t_{M=3,pine} - t_{m=1,pine})}{(t_{M=3} - t_{M=1})} \qquad \text{when } M \geq 1 \tag{6}$$

where k_1 is the growth intensity factor, $t_{M=1,\ pine}$ is the time needed for pine to reach mould index M = 1, $t_{M=1}$ is the time for the new material to reach mould index M = 1 under the same conditions as pine. M is the mould index. $t_{M=3,\ pine}$ is the time it takes for pine to reach mould index M = 3 and $t_{M=3}$ is the time it takes the new material to reach mould index M = 3.

From experiments, k_1 was found for various building materials and these were divided into four sensitivity classes, see Fig. 1. For example, pine sapwood was classified as very sensitive, spruce as sensitive and concrete as medium resistant. Aspen was not included in these experiments. The uncertainty of the model was approximated to be ± 0,5 in the mould index.

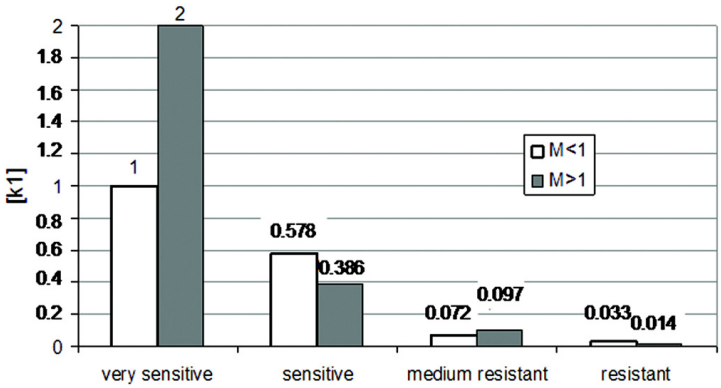

Figure 1 Sensitivity classes of the k_1 mould growth intensity factor. Pine is classified as sensitive, spruce as sensitive and concrete as medium resistant. Figure from Ojanen et al, 2010.

2.2 HYPERSPECTRAL IMAGING

Hyperspectral images are taken with specialized cameras that use a spectrograph to split light into the wavelengths it consists of, before it hits the image sensor. With this technique pictures with several hundred spectral bands, narrow wavelength ranges, can be stored. Compared to a normal RGB picture, which only stores three spectral bands, these images contain a lot more information, see Fig. 2. This information can be used to detect, for example, mould.

Before the light enters the spectrograph, it passes a thin slit, so only a narrow line of light hits the spectrograph, where it is split, and then stored to the sensor. This means it only takes pictures in one spatial direction at a time, so either the subject or the camera needs to move in the other spatial direction to obtain a two dimensional image.

Many hyperspectral cameras also include near infrared light (NIR) up to 2500nm, whereas the human eye only can see up to 700nm. With several hundred spectral bands, including infrared light, it is easier to differentiate between the materials, objects or substances in the picture, because there is a high possibility that they differ in some of the spectral bands they reflect or radiate. This differentiation requires image processing and analysis with for example PCA, partial least squares discriminant analysis (PLS-DA) or spectral angle mapper (SAM) (Burud et al 2015).

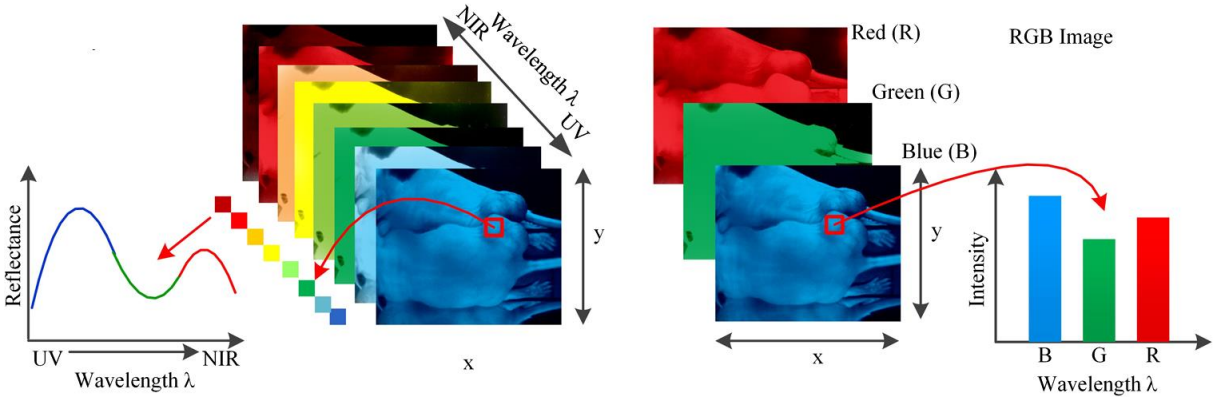

Figure 2 Hyperspectral images to the left and RGB images to the right. Each pixel in a RGB image contains three spectral bands, red, green and blue. Hyperspectral images contain up to several hundred. The graph shows a signature curve with the reflectance of the spectral bands. Figure adapted from Guolan Lu and Baowei Fei, 2013

2.3 CLIMATE

The scheffer index is “a climate-index for estimating potential for decay in wood structures above ground” – Scheffer (1970, p 25.) and has been used by several authors to make new estimates (Setliff 1986; Francis and Norton 2006). More lately Brischke et al, 2011, compared it to their decay hazard model for Europe. The Scheffer index is calculated from temperature and precipitation.

Northern Europe may expect more precipitation and higher temperature in the years to come, see Fig. 3 and Fig. 4 (van der Linden and Mitchell, 2009). Calculating future decay risk with the Scheffer index will therefore give higher risk estimates than today. Mould sets in, as mentioned earlier, quicker and in lower moisture than decay rot. Gobakken, 2010, concluded the article “Effects of climate change on mould growth”, that “moulds will most likely benefit from climate change”.

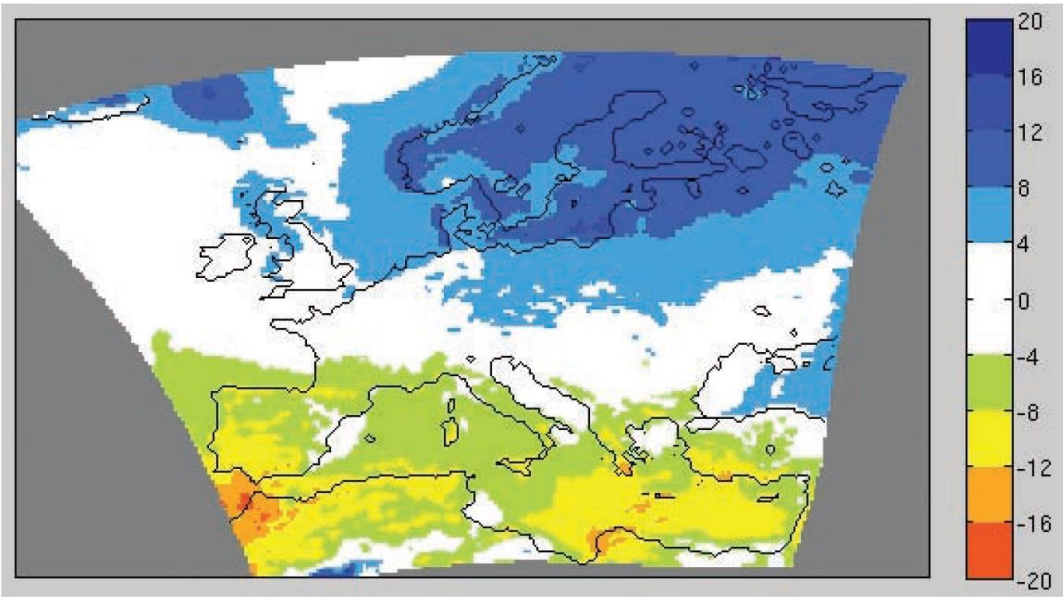

Figure 3 Projected changes in annual precipitation, in percent, for the years 2021 – 2050 compared to the 1961 – 1990 mean. From van der Linden and Mitchell, 2009, the ENSEMBLES project, A1B scenario.

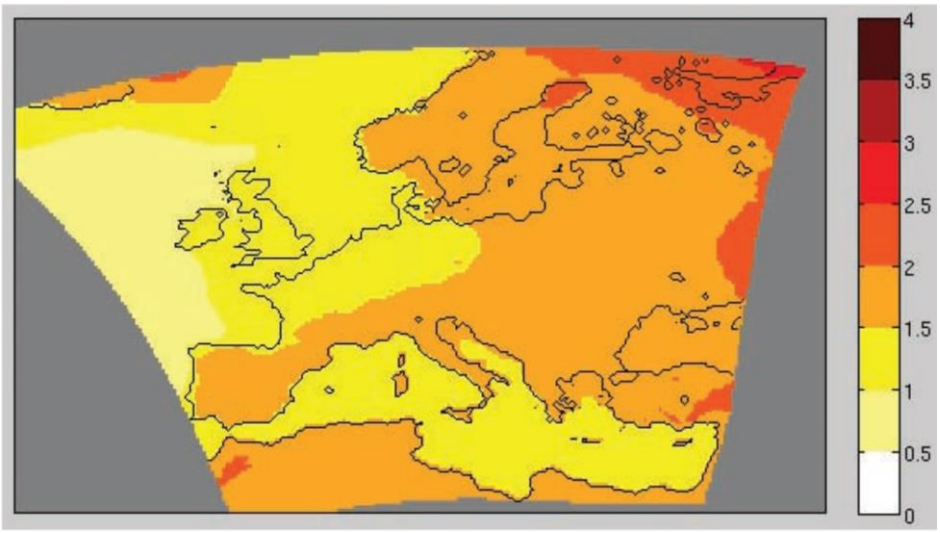

Figure 4 changes in annual mean surface air temperature, in Kelvin, for the years 2021 – 2050, compared to the 1961 – 1990 mean. From van der Linden and Mitchell, 2009, the ENSEMBLES project, A1B scenario.

Mould growth on facades, however, is not only controlled by the macroclimate, the microclimate is also a major factor. Fig. 5 shows differences of hours with condensation and wind driven rain within the same façade (Nore, 2009). The shorter condensation hours higher on the wall are mostly from less radiation loss due to the roof overhang. Small details like this can make big differences in mould growth on a façade, see Fig. 6 .

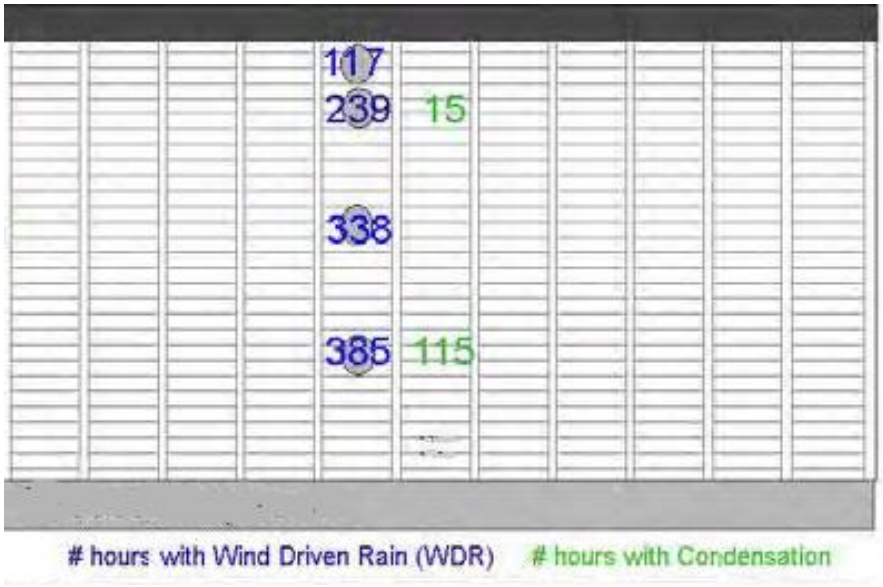

Figure 5 Wooden facade with variation in calculated hours of condensation and accumulated wind driven rain. Less condensation near the roof overhang due to less radiation loss. Adapted from Nore, 2009.

Figure 6 Ås high school. Less mould growth under the overhang.

2.4 Wood

Wood is an environmental friendly building material; it stores CO_2 and is a renewable source. Using untreated wood as outside cladding takes it a step further by not using chemicals or needing any maintenance, which also means less work and cost for the builders and the owners. Therefore, wood as an outside cladding material has increased in popularity. The aesthetic quality is also a desired factor, and this can be difficult to predict because of discolouring.

The most commonly used types of wood for cladding in Norway are pine (*Pinus sylvestris*), spruce (*Picea abies*), and aspen (*Populus tremula*). In recent years, imported wood has also been used; oak (*Quercus robur*), larch (*Larix sibirica*) and Western red cedar (*Thuja plicata*) (Larsen, 2008).

Most tree trunks have two grades of wood, sapwood and heartwood. Sapwood is closest to the bark and transports water and stores nutrients (Forest Products Laboratory, 1987, p. 2-2). Heartwood is in the middle of the trunk and no longer transports water, but stabilizes the tree. In for example pine sapwood, the nutrients and the relatively permeable and open structure which absorbs water, make it less

resistant to fungus (Øvrum and Flæte, 2008; Larsen, 2008). Pine heartwood however, is less permeable to water and contains extractives that protect against fungus, which makes it more resistant (Øvrum and Flæte, 2008). In pine, the heartwood is darker than the sapwood, but in for example aspen, they are not visually distinguishable (Walker, 1989, p. 126). There is however physical differences, Wengert showed, in 1976, a way to use the difference in permeability to distinguish the heartwood from the sapwood. An alcohol-dye mixture stained the more permeable sapwood, whilst the heartwood was unstained.

As described earlier, mould stains wood with a grey colour, and is the main factor in the colour change of wood. Dust and pollution will also grey a cladding, but another factor is degradation of lignin by sunlight (Larsen, 2008). When the lignin is oxidized by sunlight, it turns brown, this can give more colour variation to the surface of the wood.

2.5 MOISTURE TRANSPORT

In general, the transport mechanisms of moisture are vapour diffusion, surface diffusion and capillary conduction, see Fig. 7. Vapour diffusion occurs when there are differences in vapour pressure. Water vapour will diffuse from high to low vapour pressure, if the material is dry enough or not hygroscopic. Surface diffusion can occur when the material contains enough hygroscopic moisture, which is moisture held as a film of water, and is driven by relative humidity. Surface diffusion and vapour diffusion happen when the air relative humidity is up to 98%, W_{hygr}, with RH above this, capillary conduction also transports water, see Fig. 8. With constant access to water, from example rain or a leakage, capillary action continues until the saturation point, W_{max} in the same figure. Capillary conduction is driven by the surface tension and adhesive forces between the water and the material. This capillary tension can be seen as a function of the relative humidity because of the relation between capillary tension and the equilibrium humidity in the pore in front of the water surface.

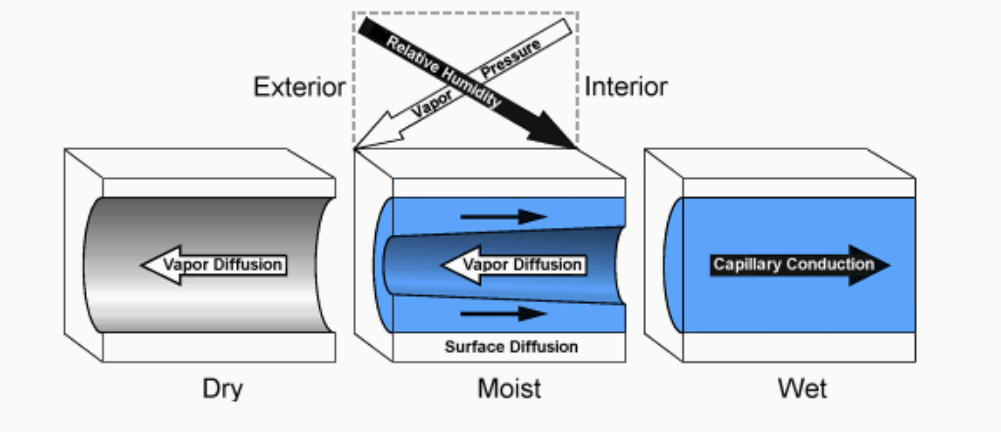

Figure 7 High relative humidity outside, high vapour pressure inside. The relationship between the three moisture transport mechanisms. Vapour diffusion from high to low vapour pressure. Surface and capillary conduction from high to low relative humidity. Figure from Fraunhofer IBP, overview of WUFI, 2009.

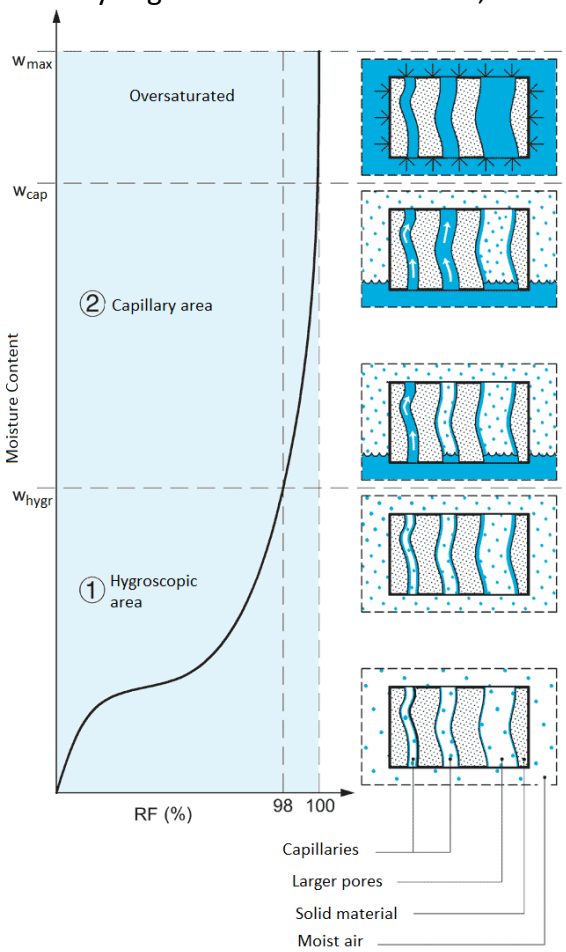

Figure 8 Moisture transport in porous materials. Pore model and sorption curve. Hygroscopic area with vapour and surface diffusion and capillary area with capillary conduction. Figure adapted from Geving, 2005.

The moisture content of wood is measured in percent of the woods dried weight. Living wood has above 30% MC, and when dried, free water in the cells evaporates

until it reaches the fibre saturation point, which for example pine, is 30% MC. When dried more, water in the cell walls dries out.

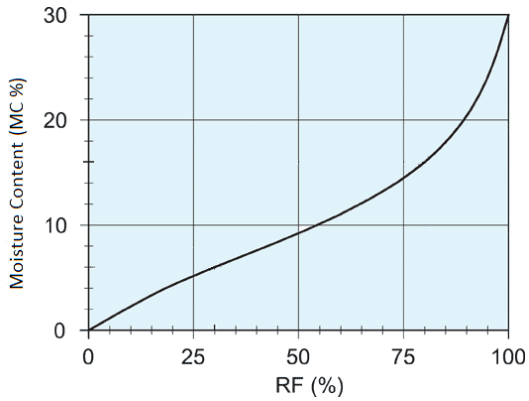

Figure 9 Sorption curve for pine wood.

Wood is hygroscopic, which means it absorbs and exudes moisture from and to the surrounding air. It reaches equilibrium moisture content when in balance with the RH of the air, the equilibrium states of a type of wood can be described with sorption curves, see Fig. 9. The cell structure of wood is built so it transports water most effectively parallel to the growth rings. Moisture content above 20%, which is the equilibrium moisture content at 80% RH, sets the wood at risk for mould attack.

3 METHODOLOGY

Wooden samples have been exposed to eight different transient climates in a laboratory. Mould growth has been measured weekly with two methods. The mould growth on aspen has been modelled with the empirical VTT model.

3.1 EXPERIMENTAL SETUP

In a laboratory, eight chambers were set up with different transient climates, see Table 3. Each chamber had a fixed temperature, relative humidity and time period of showers. Showering was simulated daily at 17:00, with one minute showering per 30 minutes in the showering period. This equals 4 x 1 min showering in the chambers with 2 hour showering and 8 x 1 min for the chambers with a 4 hour period.

Table 3 Chambers with different climates and showering periods.

Chamber	Temperature	Humidity	Period with showers
8a	10°C	65% RH	2h
8b	10°C	65% RH	4h
9A	10°C	85% RH	2h
9B	10°C	85% RH	4h
10A	25 °C	65% RH	2h
10B	25 °C	65% RH	4h
11A	25 °C	85% RH	2h
11B	25 °C	85% RH	4h

As this was part of a larger experiment, many types of wood were set up for each chamber, see Table 4. The wood samples were cut to 18*50*200 mm and sealed at each end with End Grain Sealer. A metal hook was screwed into the back of each substrate and they were hung up in rig, see Fig. 10. The order and placements of the substrates were rotated weekly.

Table 4 Wood types in each chamber

Wood type	Sapwood/Heartwood	Number of
Spruce (high density)	Heartwood	5
Spruce (low density)	Heartwood	5
Spruce (low density)	Sapwood	5
Pine	Sapwood	5
Pine	Heartwood	5
Larch	Heartwood	5
Aspen	-	5
Oak	Heartwood	5
Pine/spruce	Heat treated	5

Figure 10 Climate chamber with wood samples. Wood samples with wires logged moisture. Samples were rotated every week.

A suspension was made from three mould cultures; *Ulocladium atrum* 06/55, *Cladosporium cladosporioides* 06/54 and *Aureobasidium pullulans* BAM 9. These fungi are some of the most likely to grow in an exterior environment (NS-EN 15457:2014). The samples were sprayed with the suspension.

Differences in temperature and RH affected how long the substrates were wet after showering. Moisture, measured with a resistance humidity sensor, and temperature were continuously logged. Additionally a dielectric leaf sensor, rotated weekly between the chambers, measured moisture. Normal incandescent bulbs were used for lighting 12 hours on and 12 hours off.

3.2 HYPERSPECTRAL IMAGING

Mould on three samples each of aspen, spruce heartwood and spruce sapwood, were evaluated weekly with a hyperspectral camera, see setup Fig. 11. When handling the samples, sterile gloves were used and ffp3 masks were used whilst inside chambers to reduce the amount of mould spores breathed in. A hyperspectral camera HySpex SWIR-320i from Norsk Elektro Optikk was used for imaging. This camera has 320 pixels in width, 150 spectral bands and has a spectral range of 900 nm – 1700nm. The sample was pictured from a distance of 30 cm, which resulted in an image resolution of 3,1 pixel/mm. A translation stage moved the sample to obtain the 2D image.

Two halogen lights, one on each side, where used to provide enough lighting for the pictures. As the pictures were taken in a greenhouse, there was a high amount of natural lighting in addition to the lights. When the natural lighting was too high, shade from the sun was given by a sheet of paper. A white reference calibration plate from Specim was pictured with each substrate to correct for variations in light conditions

The program used was Hyspex GROUND 3.5, with the exposure time varying between 3500µs to 10000µs, due to varying light conditions, and frame period at 17000µs. For each week taking pictures, a new dark image was taken for each exposure time used, and automatically subtracted from the images of samples.

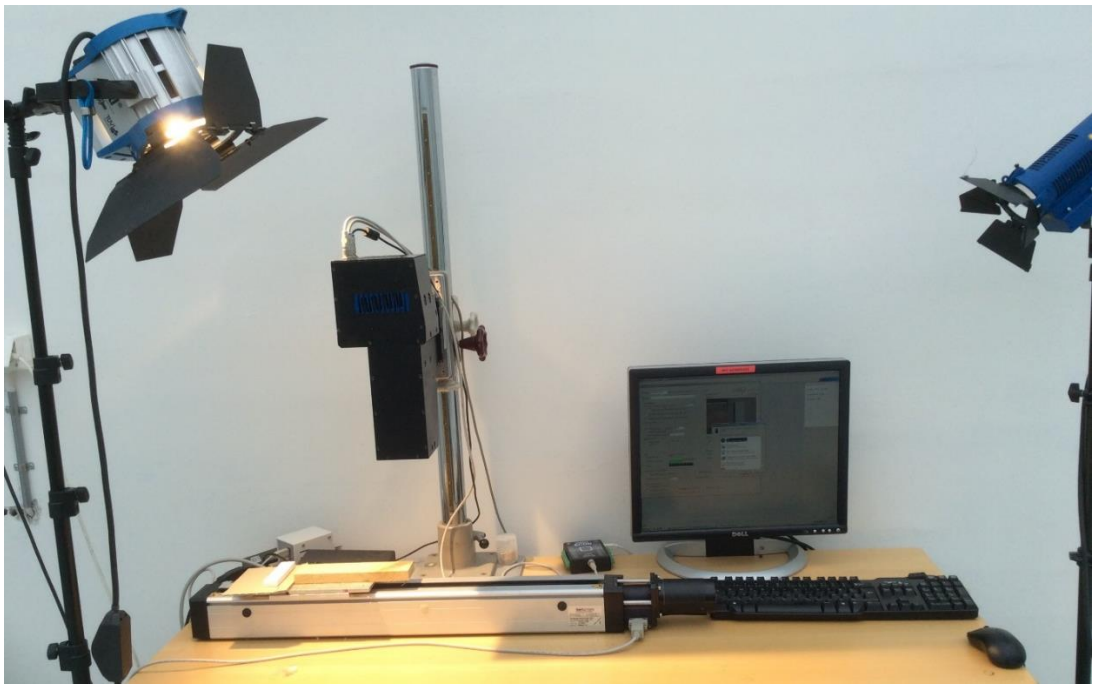

Figure 11 Hyperspectral imaging setup. Translation stage with sample and white plate on table. Hyperspectral camera 30cm above the sample and halogen lighting from above. Normally two halogen lights were used, one on each side.

The hyperspectral images were analysed in Matlab with MIA and PLS toolboxes from Eigenvector. A script written by a team at IMT, NMBU read the Hyspex files into Matlab. First, the white balance was fixed by dividing each pixel with the average pixel on the white plate, this was done with a script also written the team at IMT, NMBU. The pictures were then cropped to include only the wooden cladding. A sample with visible fungus was chosen to make a model with PLSDA (Vinzi et al, 2010). Within an area with clearly visible mould, a small selection was classified as mould. In the same way selections within areas without visible mould were classified as wood. These selections act as references for mould and wood, so the program can predict what is mould and what is wood in other pictures. This technique is called supervised classification. Pre-processing was set to mean centre and autoscale and the model was processed. This mould model was utilized to make the prediction models for all other samples. The prediction probability for the class mould, gave a black and white picture, mould as white, wood as black, which was stored as a .tiff image and further processed in Fiji ImageJ (Schindelin et al., 2012). In Fiji, Otsu (Otsu, 1979) auto threshold was applied to each picture and the percentage of white area

was estimated. Excel was utilized to make graphs of the mould growth from the percentages obtained.

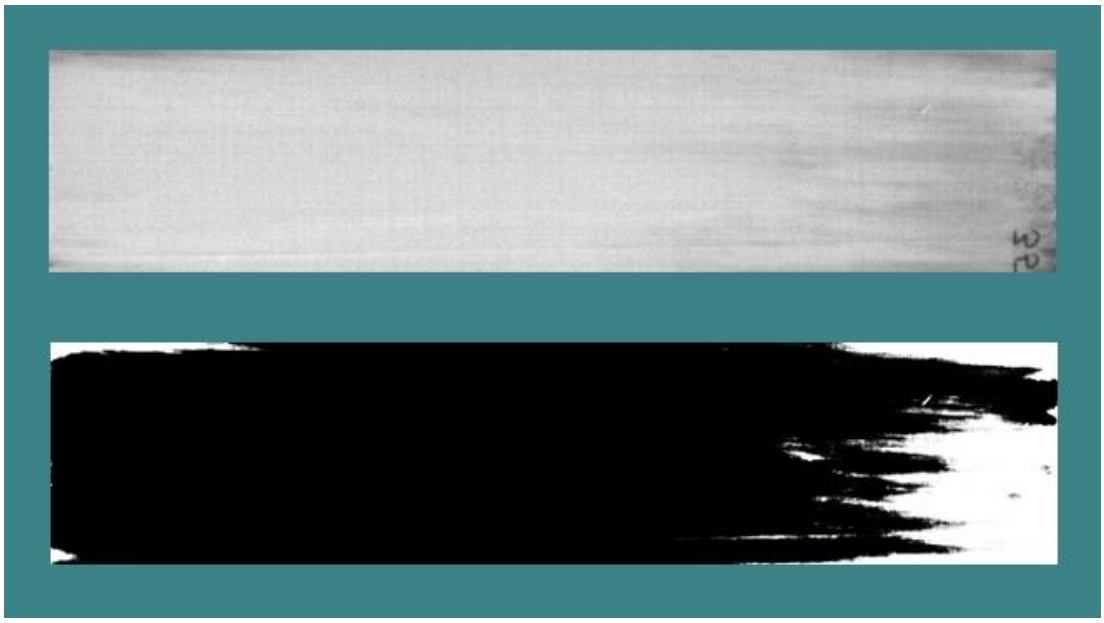

Figure 11 Hyperspectral image in greyscale on top, after PLS-DA processing showing mould white and wood black, bottom. Sample 35 after 7 weeks was estimated with Fiji to have 13% mould coverage.

3.3 VISUAL ASSESSMENT VS HIM

Visual assessment was done by fellow students with a slightly modified version of NS-EN 16492:2014, table A.3, see table 1 in this paper. When rating 4, an estimation of percentage was noted in addition to the rating, for example: rating 4, 85% coverage. Also, when mould was only visible with a magnifying glass, it was denoted [1] and used as an approximation of $t_{M=1}$.

To compare HIM and visual assessment method the mould ratings have been converted by using the average percentage of each rating, see Table 5. Uncertainties equal the percentage range in the rating, except for rating 4 when an estimation of percentage has been made, the uncertainty is assumed to be up to 10 percentage points.

Table 5 Rating conversion. The average percentage used to compare HIM to visual assessment graphs in the rightmost column.

Mould Rating	Percentage area of disfigurements (NS-EN 16492:2014)	Average percentage
0	0	0
1	Up to 10%	5%
2	10% to 30%	20%
3	30% to 50%	40%
4	50% to100%	75% or estimated value

3.4 THE VTT MODEL

The VTT model described has been tested with conditions and results from chamber 9A. An Excel spreadsheet from Viitanen calculated all necessary values, k_2 from eq. (2) and M_{max} from eq. (3), with A = 1, B = 7, C = 2. The duration of time the surface of the samples were wet, was calculated in the model as 100% RH. The number of hours the surface was wet was estimated from the dielectric leaf wetness sensor, see Fig. 13. With a threshold of 350mV, the sensor was wet 8 hours the fourth week, and 3 hours two months later in chamber 9A, see Fig. 33. This was approximated to six hours 100% RH. RH_{crit} was calculated with eq. (4), with T = 10°C. The mould growth rate, $\frac{dM}{dt}$ was calculated from eq. (1), with T = 10°C, SQ = 0 and W = 0. The growth intensity factor, k_1, was calculated from the visual ratings for pine and aspen with equations (5) and (6). This was done by taking the averages of $t_{M=1,\ pine}$ and $t_{M=3,\ pine}$ from five samples of pine and the averages of $t_{M=1}$ and $t_{M=3}$ from four samples of aspen.

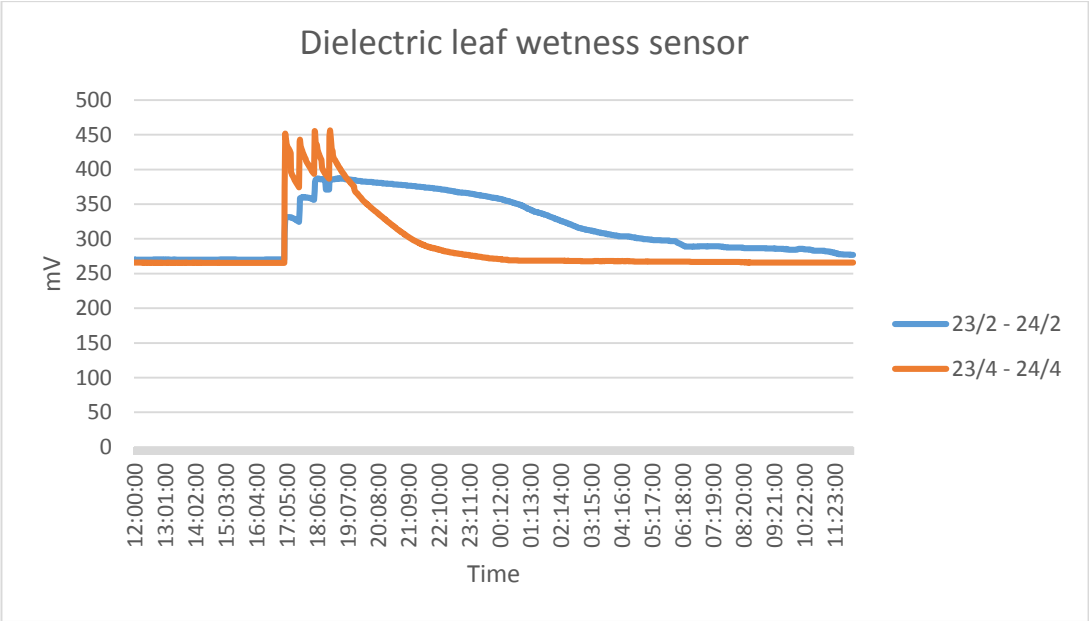

Figure 23 Dielectric leaf wetness measured the 23/2 -24/2 and two months later, 23/4 -24/4 in chamber 9A. The showering started at 17:00 each day, which can be seen by the spike in mV.

3.5 Uncertainties

The uncertainty in k_1, δk_1, when $M < 1$ and uncertainties in $t_{M=1}$ and $t_{M=3}$ for pine and aspen assumed independent and random, was calculated with the formula:

$$\frac{\delta k_1}{|k_1|} = \sqrt{\left(\frac{\delta \overline{t_{M=1,pine}}}{\overline{t_{M=1,pine}}}\right)^2 + \left(\frac{\delta \overline{t_{M=1,aspen}}}{\overline{t_{M=1,aspen}}}\right)^2} \quad (7)$$

where δk_1 is the uncertainty in k_1 when $M < 1$ and k_1 is the mould growth intensity factor. $\delta \overline{t_{M=1,x}}$ is the uncertainty in $\overline{t_{M=1,x}}$, and $\overline{t_{M=1,x}}$ is the average of $t_{M=1,x}$ where x indicates pine or aspen. $t_{M=1}$ is the time it takes to reach mould index 1, see eq. (5) and (6). The uncertainty $\delta \overline{t_{M=1,x}}$ was calculated as the standard deviation of the mean:

$$\delta \overline{t_{M=1,x}} = \frac{\sigma_{t_{M=1,x}}}{\sqrt{N}} \quad (8)$$

here, $\delta \overline{t_{M=1,x}}$ is the uncertainty in $\overline{t_{M=1,x}}$, $\sigma_{t_{M=1,x}}$ is the standard deviation of $t_{M=1,\,x}$ and N is number of measured samples, five for pine and four for aspen. x indicates

pine or aspen. The uncertainty $\sigma_{t_{M=1,x}}$ was calculated with the sample standard deviation:

$$\sigma_{t_{M=1,x}} = \sqrt{\frac{\sum_{i=1}^{N}\left(t_{M=1,x_i} - \overline{t_{M=1,x}}\right)^2}{N-1}} \tag{9}$$

Where $\sigma_{t_{M=1,x}}$ is the standard deviation of $t_{M=1,x}$ and $t_{M=1,x_1}$, $t_{M=1,x_2}$,…… $t_{M=1,x_N}$ are the measured times for the samples to reach mould rating 1. $\overline{t_{M=1,x}}$ is the average of $t_{M=1,x}$, N is number of samples and x denotes pine or aspen.

For $M > 1$, the uncertainty in k_1, assumed the uncertainties in $t_{M=1}$ and $t_{M=3}$ were independent and random, was calculated with:

$$\delta k_1 = \sqrt{\begin{array}{c}\left(\frac{2\cdot\delta t_{M=3,pine}}{\left(t_{M=3,aspen} - t_{M=1,aspen}\right)}\right)^2 + \left(\frac{-2\cdot\delta t_{M=1,pine}}{\left(t_{M=3,aspen} - t_{M=1,aspen}\right)}\right)^2 + \\ \left(\frac{-2\cdot\left(t_{M=3,pine} - t_{M=1,pine}\right)\cdot\delta t_{M=3,aspen}}{\left(t_{M=3,aspen} - t_{M=1,aspen}\right)^2}\right)^2 + \\ \left(\frac{2\cdot\left(t_{M=3,pine} - t_{M=1,pine}\right)\cdot\delta t_{M=1,aspen}}{\left(\delta t_{M=3,aspen} - \delta t_{M=1,aspen}\right)^2}\right)^2\end{array}} \tag{10}$$

Where δk_1 is the uncertainty in k_1 when $M > 1$, $t_{M=3,pine}$ is the time it takes for pine to reach mould index 3 and $\delta t_{M=3,pine}$ is the uncertainty in $t_{M=3,pine}$. $t_{M=1,pine}$ is the time it takes for pine to reach mould index 1 and $\delta t_{M=1,pine}$ is the uncertainty in $t_{M=1,pine}$. $t_{M=3,apen}$ is the time it takes for aspen to reach mould index 3 and $\delta t_{M=3,aspen}$ is the uncertainty in $t_{M=3,aspen}$. $t_{M=1,aspen}$ is the time it takes for aspen to reach mould index 1 and $\delta t_{M=1,aspen}$ is the uncertainty in $t_{M=1,aspen}$

4 RESULTS

4.1 HYPERSPECTRAL IMAGING

Mould growth, in percentage of surface covered, from the hyperspectral imaging method (HIM) described, using Matlab and Fiji for image processing and Excel for graphs, are shown in Fig. 14, 15, 16 and 17. In chambers 8A, 8B, 10A and 10B, see Table 3 in methodology, HIM did not detect any mould growth after 7 weeks. Mould growth on spruce sapwood and heartwood was also too little to detect.

HIM, in chamber 9A, Fig. 14, with climate conditions 10°C, 85% RH and 2 hours of light showers, showed up to 85% surface coverage after 11 weeks, and sample 47 showed no mould growth.

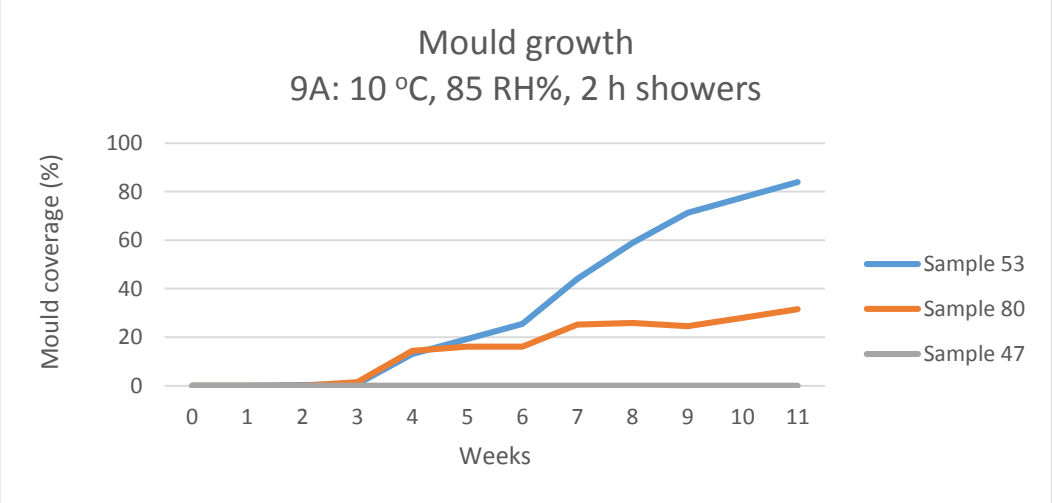

Figure 14 Mould growth curves from hyperspectral images of untreated aspen in laboratory climate of 10 degrees Celsius, 85% relative humidity and 2 hours of daily showers. Shows percentage of surface covered with mould.

In chamber 9B with climate conditions 10°C, 85% RH, 4 hours light showers, HIM showed up to 100% percent mould coverage after 4 weeks, and on sample 238, no growth after 11 weeks, see Fig. 15.

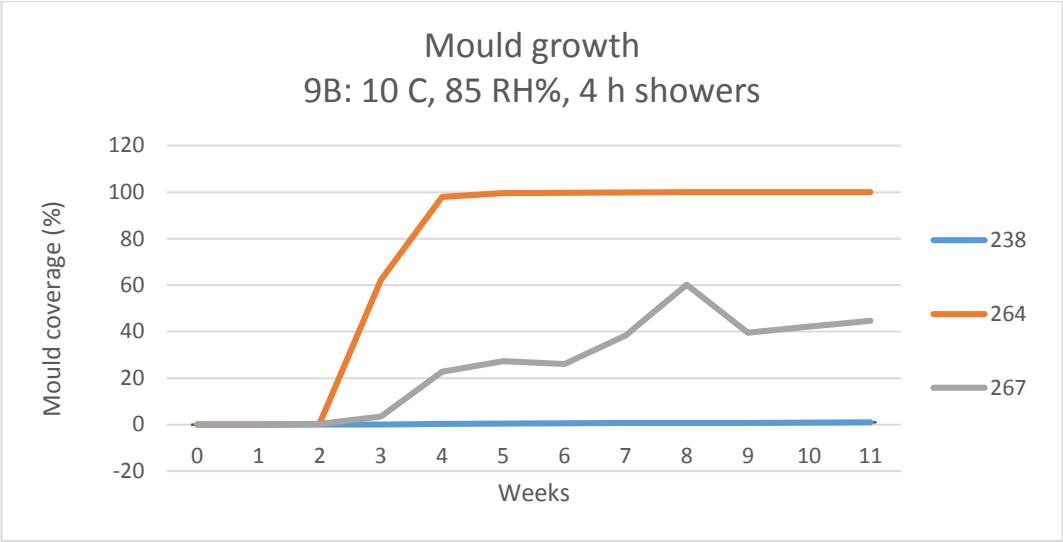

Figure 15 Mould growth curves from hyperspectral images of untreated aspen in laboratory climate of 10°C, 85% relative humidity and 4 hours of daily showers. Shows percentage of surface covered with mould.

In chamber 11A, HIM showed up to 85% mould coverage after 7 weeks and no growth on sample 12, see Fig. 16.

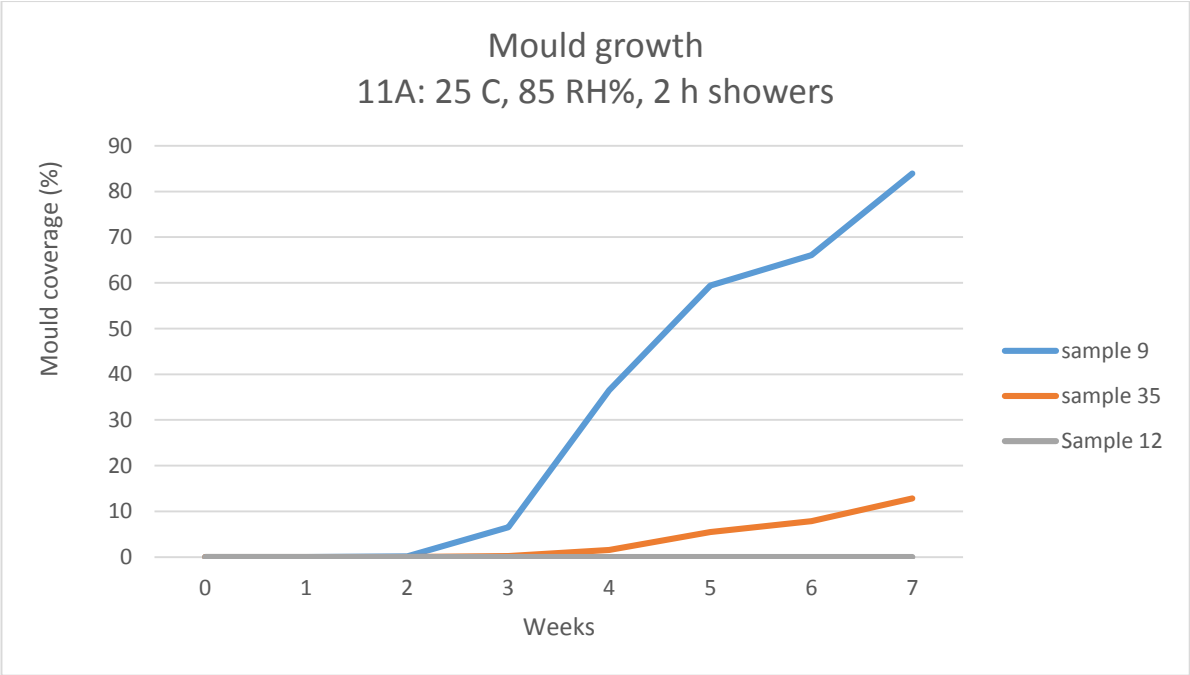

Figure 16 Mould growth curves from hyperspectral images of untreated aspen in laboratory climate of 25 degrees Celsius, 85% relative humidity and 2 hours of daily showers. Shows percentage of surface covered with mould.

In chamber 11B HIM showed up to 100% mould coverage after 4 weeks and one sample with no growth, see Fig 17.

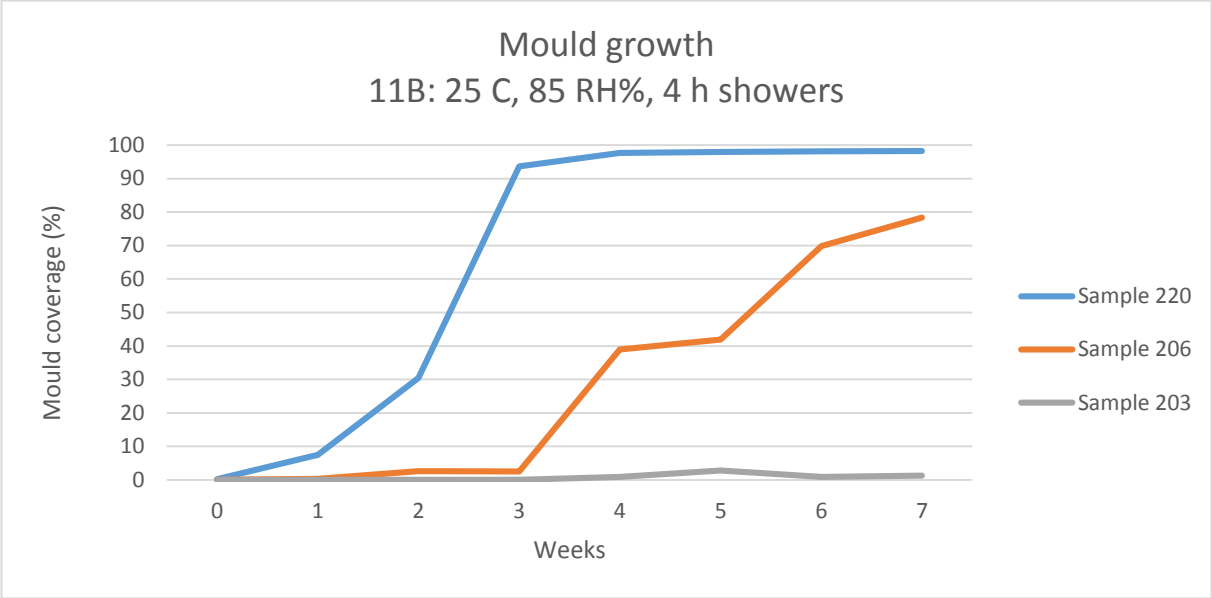

Figure 17 Mould growth curves from hyperspectral images of untreated aspen in laboratory climate of 25°C, 85% relative humidity and 4 hours of daily showers. Shows percentage of surface covered with mould.

4.2 VISUAL ASSESSMENT

Mould indexes from visual assessment method have been converted to percentages as shown in Table 5. Uncertainties are assumed to be up to 10 percentage points for the visual method. Below are graphs comparing HIM with visual assessment of one sample from each chamber. Sample 53 shows a difference between HIM and visual assessment of approximately 20 percentage points after 9 weeks, see Fig. 18.

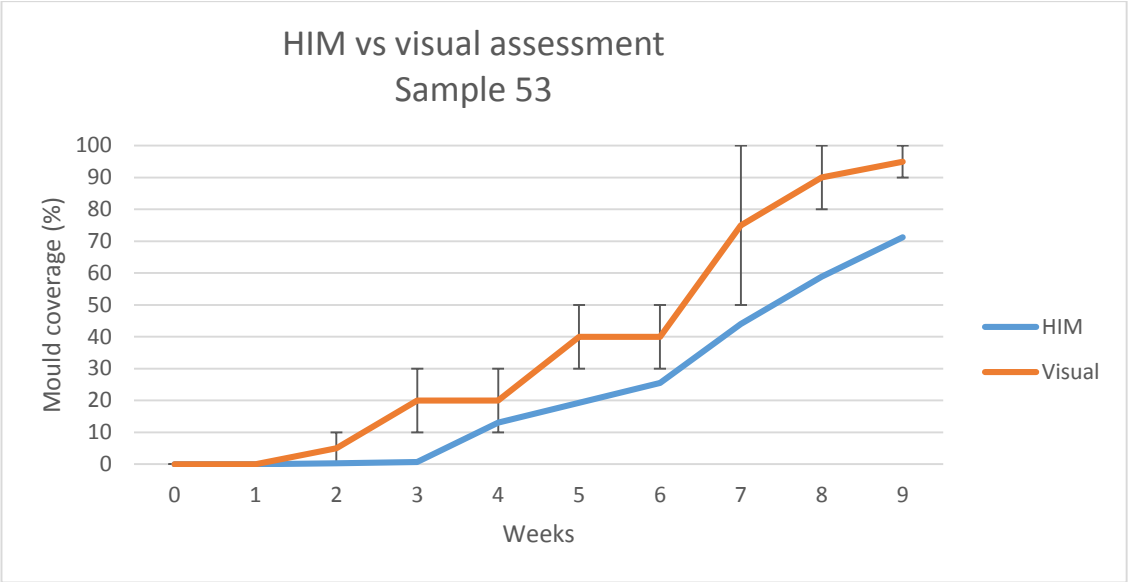

Figure 18 Hyperspectral imaging and visual assessment mould growth curves for sample 53 from chamber 9A.

Sample 267 from chamber 9A has a noticeable hump in week eight from the HIM method only, see Fig. 19, and has up to 55 percentage points difference compared with visual assessment.

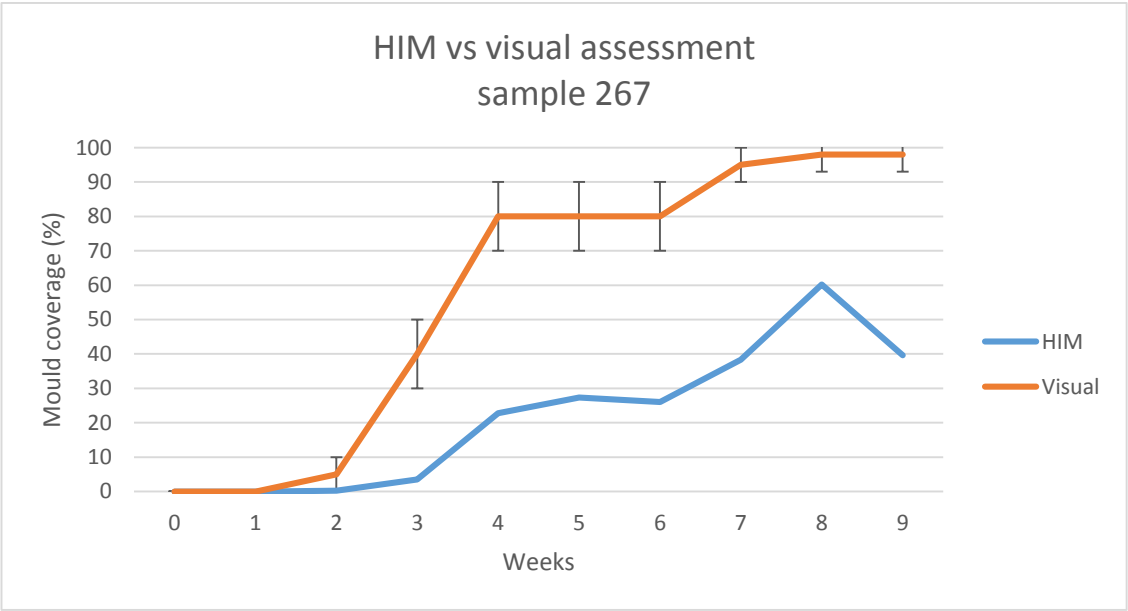

Figure 19 Mould coverage with HIM and visual assessment for sample 267 from chamber 11A, shows up to 55 percentage points in difference.

Sample 35 in chamber 11A, and sample 206 in chamber 11B, HIM showed up to 30 percentage points less than visual assessment method, see Fig. 20 and 21.

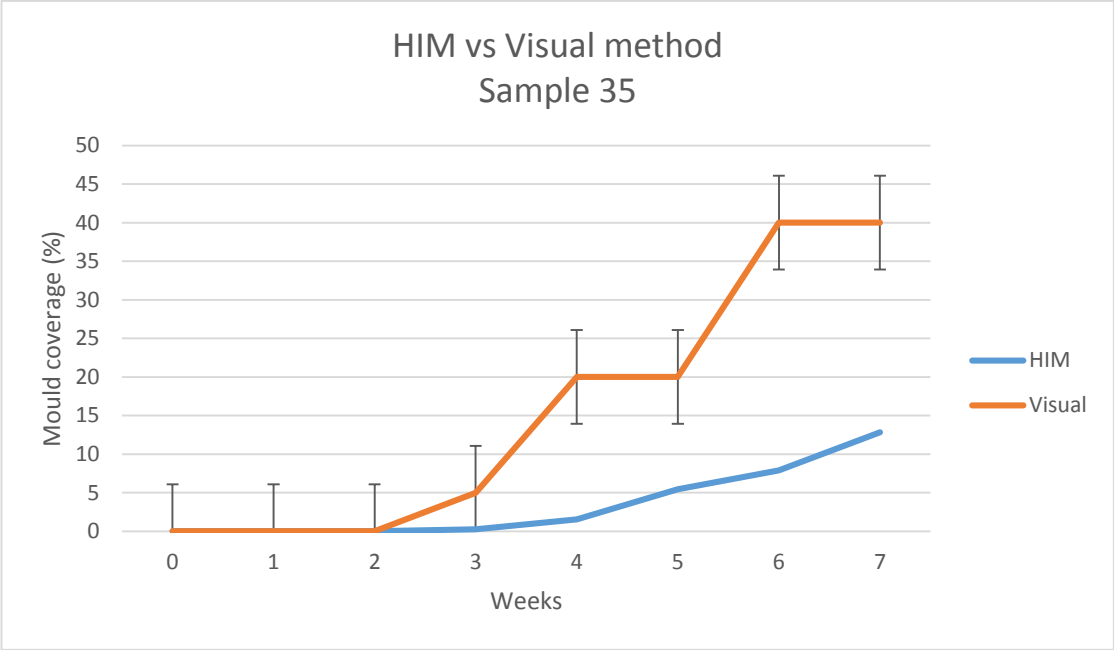

Figure 20 Mould coverage with HIM and visual assessment for sample 35 shows up to 30 percentage points in difference.

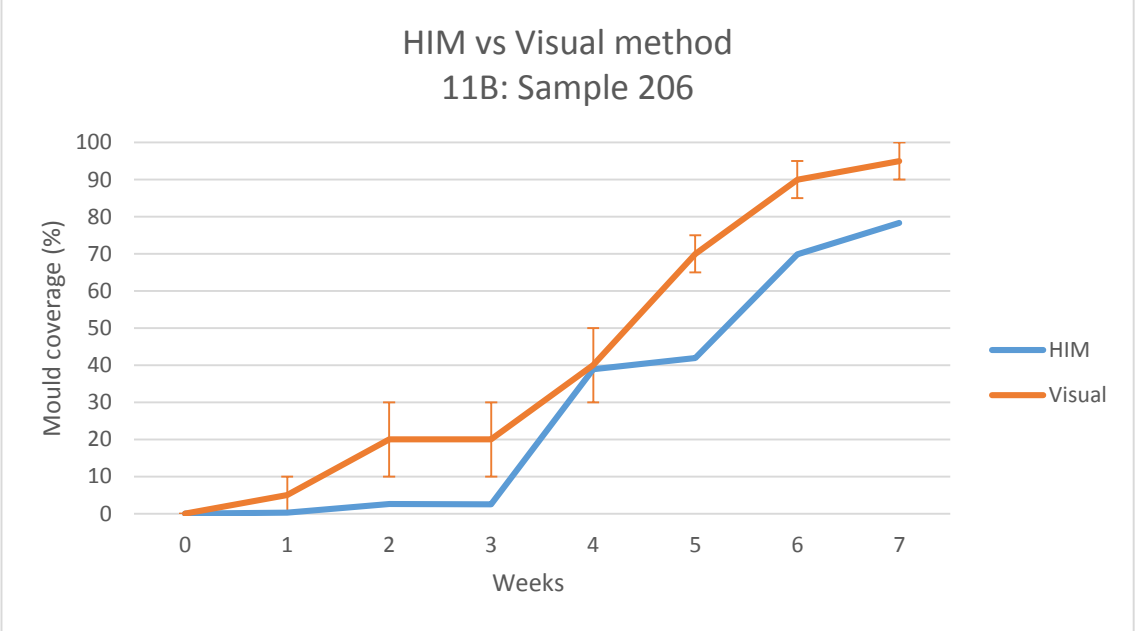

Figure 21 Mould coverage with HIM and visual assessment for sample 206 shows up to 30 percentage points in difference.

4.3 HYPERSPECTRAL IMAGING VS MODEL

The k_1 factor for aspen in chamber 9A was calculated to be k_1 = 10 ±10 with (5) and (6) and with uncertainties from equations (6) and (9) for M > 1. For M < 1, k_1 = 0,9 ± 0,2 with equations In calculations for the model however, k_1 = 6,4 has been used. The mould growth was then calculated with equation (1) and is presented in Fig. 22 together with the curves for HIM and visual assessment, which are the averages of the three samples in chamber 9A.

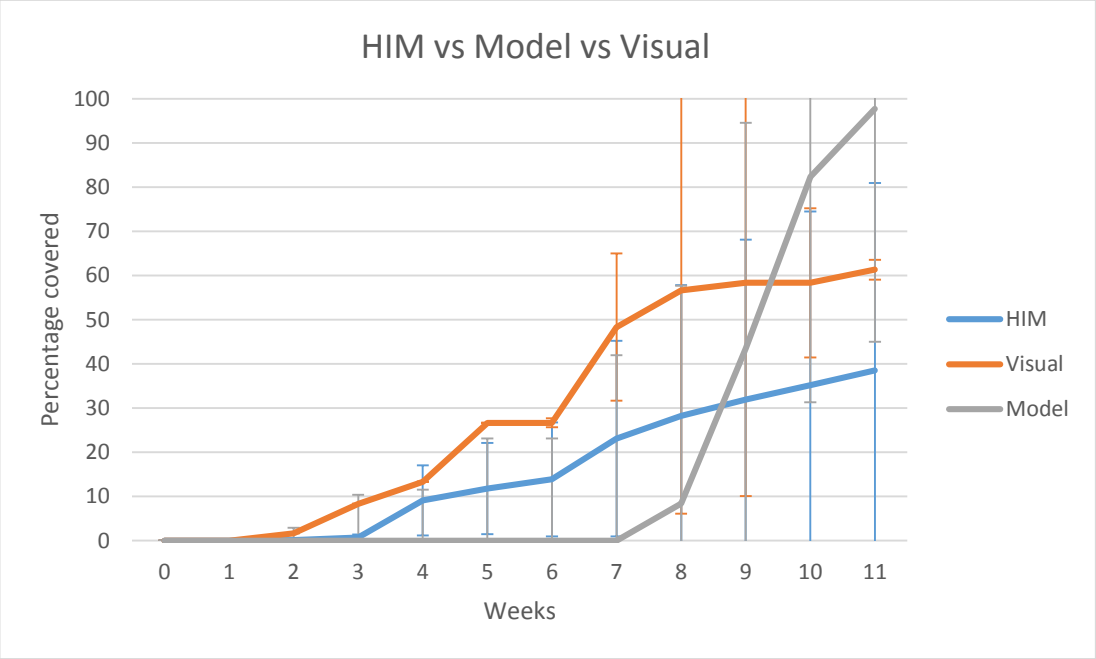

Figure 22 Mould growth model for aspen in climate conditions 10°C, 85% RH and 2 hours showering, compared to measured mould growth by HIM and visual assessment.

Calculations of k_1 for chambers 9B, 11A and 11B was not possible because of insufficient data.

5 DISCUSSION AND CONCLUSION

The hyperspectral imaging method has consequently shown less mould than by visual assessment. In Fig. 19, sample 267, week 8, there is a bump in the percentage of mould, from 40% to 60% down to 40% again. Considering the visual evaluation is approximately the same in week 7, 8 and 9, and no noted decline of mould on the sample, this bump is regarded as an error. This means the uncertainty can be up to 20/40 x 100% = 50%. This is an extreme case but gives an indication of the uncertainty. For hyperspectral imaging to be useful, it should be accurate, and this I believe, is not accurate enough.

The method used was not entirely objective. When making the PLS-DA model using the supervised classification technique, areas of mould were chosen to represent the mould. How big, and which areas sampled as mould made a difference to the percentage of mould estimated.

Though the HIM used in this study neither gave a very accurate or entirely objective assessment, it may have potential as a mould assessment tool on wooden cladding.

The adaptation of the VTT model to aspen worked, although not accurate. The growth intensity factor for aspen found of k_1 = 10 ±10 has such a large uncertainty, its value is questionable. Which sensitivity class, see Fig. 1, aspen belongs to, is not determinable with this accuracy.

5.1 CRITICAL ASSESSMENT

As described, the HIM gave up to 50% error. This specific instance, sample 267, see Fig. 19, is most likely to be from light issues. Clouds passing by in a blue sky, during taking a picture, could result in the picture being darker on one side. Normally, a new picture was taken, but not every time was noticed. The light conditions also changed from week to week. An even and equal exposure each time proved difficult. These

shifting light conditions are the main source of error for the HIM. The white reference plate did counteract some of these shifting light conditions, but also this may be a source of error, as it might not be perfectly white.

The image analysis may also have introduced some error. As mentioned, the objectivity was not absolute. In addition, when selecting areas to represent wood, with the picture quality in Fig. 12, there may have been mould in the area classified as wood. This may have lead to a smaller estimate of mould, as some mould would be regarded as wood. Using more time in this stage, with the supervised classification and with different types of pre-processing, may give results that are more accurate.

The aspen wood samples were homogenous in colour and almost without visible growth rings. This made it quite easy to distinguish the mould from the wood and in this case, a normal RGB may be equally as good as hyperspectral images. Pine and spruce however often have more visible growth rings, which are darker than the surrounding wood, this would most likely make it difficult for a RGB image to separate the mould from the growth rings. In addition, this was an indoor experiment without other degradation from outside elements. Outdoors, lignin degradation may make it more difficult for a RGB image to differentiate between the mould and the wood.

The high variation in mould coverage within the same chambers for aspen was one of the reasons for the high uncertainty in k_1. This variation may be due to no differentiation between heartwood and sapwood of aspen. There is a difference in permeability, as earlier described, which may give a longer time of wetness for the more permeable sapwood, which would result in heavier mould growth.

The other, and likely largest, source of error in k_1, is the approximation of using mould index [1] as $t_{M=1}$. In the VTT model $t_{M=1}$ is the time in days it takes until small amounts of mould are visible with a microscope on the surface. The method used in this study, used only magnifying glasses, at best, to detect mould, which means that $t_{M=3}$ is approximately the same as $t_{M=1,}$ or that in fact, no $t_{M=1}$ was measured. In chamber 9A however, growth was slow enough to differentiate more between stages of growth, which gave a more reliable mould index [1]. The equations (5) and (6) are fractions, so if both $t_{M=1,pine}$ and $t_{M=1,aspen}$ were equally shorter, the approximation may not have

very large consequences. Some samples had no initial stage [1], but went from mould index 0 to 1, or 2, within a week, $t_{M=3}$ was then used as $t_{M=1.}$ These increased the error largely and could have been excluded. Another major flaw, $t_{M=1}$ is measured in days, whilst the method used only measured weekly. For a more accurate k_1, microscopes must be used and mould growth must be measured more often.

The time with 100% RH was an approximation from the dielectric leaf sensor measurements. This is also a source of error. How the wetness of the leaf sensor corresponded to the wetness of the surface of the wood, was not known. The VTT model is not developed for use with simulations of rain, and does not take into account the moisture content of the wood. The moisture content is simulated by the RH, which may be a weakness. As seen in Fig. 23, the wetness time changed over the two months, why this happened or if it is an error is unknown. If it is correct, the time the wooden surface is wet is a variable with time, it decreases over the two months. This may give less rise in the model curve in Fig. 22. Pine sapwood and aspen are assumed to be fairly similar in resistance to mould, with a k_1 =2 for aspen, the model curve would have even less rise

5.2 CONCLUSION

Mould and untreated aspen have differences in reflectance and/or radiation in the wavelength area of 900nm – 1700nm. This can be used to measure amount of mould on an untreated aspen cladding with hyperspectral cameras. The light conditions may be important for accuracy. With technological advancements in cameras, this method may become a quick and easy mould assessment method.

Higher accuracy is needed to estimate the sensitivity class of aspen, by use of microscope and daily mould assessments.

6 BIBLIOGRAPHY

Adan, O. C. G. (1994). *On the fungal defacement of interior finishes*. Thesis, Eindenhoven University of Technology, Eindenhoven.

Bardage, S.L., 2004. Assessment of mould growth. In: COST E18 e Symposium on Measurement Methods, 16e17 February, Copenhagen, Denmark. COST Secretariat,EU, Brussels.

Brischke, C., Hansson, E. F., Kavurmaci, D., Thelandersson, S., (2011) *Decay hazard mapping for Europe.* Leibniz University Hannover, Lund University

Burud, I., Gobakken, L.R., Flø, A., Thiis, T.K., Kvaal, K. (2015) *Hyperspectral near infrared imaging of wooden surfaces performed outdoors and indoors.* NIR news, Vol. 26, No 1

Burud, I., Gobakken, L.R., Flø, A., Kvaal K., Thiis, T.K. (2013) *Hyperspectral imaging of blue stain fungi on coated and uncoated wooden surfaces*, Int. Biodeter. Biodegr. 88, 37–43

Cochrane, V. (1958) *Physiology of Fungi*. John Wiley and Sons, Inc, New York.

Edvardsen, K. I., Ramstad, T. (2012). T*rehus*. *Håndbok 53*. Oslo. 333 s. s

EN 927-3 (2000) *Paints and varnishes—coating materials and coating systems for exterior wood—part 3. Natural weathering test*. European Committee for Standardization

EN 16492:2014 *Paints and varnishes. Evaluation of the surface disfigurement caused by fungi and algae on coatings.* Norsk standard, Lysaker

Forest Products Laboratory, (1987). *Wood handbook: Wood as an engineering material*. Washington, DC: US Department of Agriculture, 466 p.

Francis, LP, Norton, J (2006). *Predicting the decay resistance of timber above-ground. 1. Climate effects*. Document IRG/WP 06-20330. International Research Group on Wood Protection, Stockholm

Fraunhofer IBP(2009). *Moisture Transport In Building Materials Computer. Simulation with the WUFI Model.* http://www.wufi.de/wufi/grundl_ueberblick_e.html

Hukka, A. & Viitanen, H. (1999). *A mathematical model of mould growth on wooden material*. Wood Science and Technology, 33(6):475–85.

Geving, S. (2005). *Fukt i bygninger. Teorigrunnlag.* Byggforsk, Oslo.

Gobakken, L. R., (2010). *Effects of global climate on mould growth- interactions of concern.* IRG/WP 10-50270, Ås

Guolan Lu and Baowei Fei (2013). *Medical hyperspectral imaging: a review.* Journal of Biomedical Optics. Vol. 19, Issue 1, Atlanta

Larsen, K. E. (2008). *Kledninger av ubehandlet tre*. 542.645. Byggforsk, NTNU

Magnussen, K. (2007). *Råte- og fargeskadesopp. Skadetyper og utbedring.* 720.082. Byggforsk, Oslo

Mattson, J. (2004). *Muggsopp i bygninger. Forekomst, påvisning og utbedring.* Mycoteam, Oslo

Nore, K., Thue, J.V. and Rydock, J.P. (2006) *A comparison of time-of-wetness and wind-driven rain measurements on wooden cladding*. Proceedings of the 5th International Conference on ColdClimate - Heating, Ventilation and Air-Conditioning, Moscow, Russia.

Otsu N. (1979), *A threshold selection method from gray-level histogram*, IEEE Transaction on Systems, Man and Cybernetics, Vol 9, NO. 1, P. 62-66

Ojanen, T., Viitanen, H. et al (2010). *Mold growth modeling of building structures using sensitivity classes of materials*. Ashrae, Finland

Scheffer, T. C., (1970). *A climate index for estimating potential for decay in wood structures above ground.* Forest products journal, Vol. 21, No. 10.

Schindelin, J.; Arganda-Carreras, I. & Frise, E. et al. (2012), *Fiji: an open-source platform for biological-image analysis*, *Nature methods* 9(7): 676-682

Sedlbauer, K. (2002*). Prediction of mould fungus formation on the surface of and inside building components*. Thesis, Holzkirchen, Germany.

Setliff, EC (1986): *Wood decay hazard in Canada based on Scheffer‟s climate index formula*. The Forestry Chronicle (October): 456-459.

Thelandersson, S. Isaksson, T. (2013). *Mould resistance design (MRD) model for evaluation of risk for microbial growth under varying climate conditions.* Building and environment 65, 18 – 25, Lund

Van den Bulcke, J., Van Acker, J., Stevens, M., (2006). *Assessment of blue-stain resistance according to the EN 152 and a reverse test method using visual and computeraided techniques.* Int. Biodeterior. Biodegrad. 57, 229-238.

Van den Bulcke, J., Van Acker, J., Stevens, M., (2005). *Image processing as a tool for assessment and analysis of blue stain discoloration of coated wood*. Int. Biodeterior. Biodegrad. 56, 178-187.

Van der Linden P., and J.F.B. Mitchell (eds.) (2009) *ENSEMBLES: Climate Change and its Impacts: Summary of research and results from the ENSEMBLES project.* Met Office Hadley Centre, FitzRoy Road, Exeter EX1 3PB, UK. 160pp.

Vinzi, V., Chin, W.W., Henseler, J. et al., eds. (2010). *Handbook of Partial Least Squares*

Viitanen, H. (1994). *Factors affecting the development of biodeterioration in wooden constructions.* Materials and Structurese, 27, p 483 – 493

Walker, A. (1989). *The encyclopedia of wood*. London, Quarto Publishing plc, 192 p.

Wengert, E. M. (1976). *A quick method to distinguish aspen heartwood and sapwood.* Wood and fiber, V. 8(2)

Zabel, R. A. and Morrell, J. J. (1992). *Wood microbiology: decay and its prevention.* San Diego, Academic Press, Inc. 476 p.

Øvrum, A., Flæte, P. O. (2008). *Kjerneved av furu.* Fokus på tre. Nr. 25. Norsk Treteknisk Institutt, Oslo

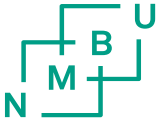

Norwegian University
of Life Sciences

Postboks 5003
NO-1432 Ås, Norway
+47 67 23 00 00
www.nmbu.no